Türk Bilim ve Mühendislik Dergisi
Turkish Journal of Science and Engineering

Analysis of MHD Richardson Flow Past An Exponentially Stretched Infinite Plate with Suction and Cross-Diffusion Effects

Uchenna Awucha UKA[1]* , **Promise MEBINE[2]** , **Samson Ademola AGUNBIADE[1]**

[1]Babcock University, School of Science and Technology, Department of Basic Sciences-Ogun State-Nigeria
[2]Niger Delta University, Department of Mathematics-Wilberforce Island-Bayelsa State-Nigeria
*Corresponding Author: ukau@babcock.edu.ng

ARTICLE INFO	ABSTRACT
	The present paper investigate the effects of magnetic field (MHD), Richardson and suction on an exponentially expanded infinite plate by studying the convective heat and mass transfer of a non-Newtonian incompressible viscous and electrically conducting fluid. Cross-diffusion impacts are also taken into consideration. The governing partial differential equations (PDEs) are transformed into ordinary differential equations through the application of well-posed similarity transformation variables (STVs). Thus, the transformed dimensionless equations are solved analytically by integrating factor approach and the resulting solutions are simulated with an efficient stability numerical algorithm known as Mathematica. The results are displayed in tabular and graphical forms while the effects of various parameters on the velocity, temperature, concentration, skin–friction coefficient, Nusselt and Sherwood numbers are discussed in details. It was found that velocity falls when magnetic field and suction parameters increase. Also, the temperature and nanoparticle concentration decreases as suction number rises but are enhanced as diffusion-thermo and thermal-diffusivity parameters rise. An increase in Richardson and Prandtl numbers leads to a decrease in skin-friction and upsurge in the rate of heat transportation. The results of this study can be used to advance the design, operation, and performance of various systems encountered in industrial and scientific applications.

MHD Richardson Akışının Emiş ve Çapraz Difüzyon Etkileri ile Üstel Olarak Gerilmiş Sonsuz Bir Plakadan Geçmesinin Analizi

MAKALE BİLGİSİ	ÖZET
	Bu makale, Newtonyen olmayan sıkıştırılamaz viskoz ve elektriksel olarak iletken bir akışkanın konvektif ısı ve kütle transferini inceleyerek, manyetik alanın (MHD), Richardson ve emmenin üstel olarak genişleyen sonsuz bir plaka üzerindeki etkilerini araştırmaktadır. Çapraz difüzyon etkileri de dikkate alınır. Geçerli kısmi diferansiyel denklemler (PDE'ler), iyi konumlanmış benzerlik dönüşüm değişkenlerinin (STV'ler) uygulanması yoluyla sıradan diferansiyel denklemlere dönüştürülür. Böylece, dönüştürülen boyutsuz denklemler, entegre faktör yaklaşımıyla analitik olarak çözülmekte ve elde edilen çözümler, Mathematica olarak bilinen etkin kararlılık sayısal algoritmasıyla simüle edilmektedir. Sonuçlar tablo ve grafik formlarında gösterilirken, çeşitli parametrelerin hız, sıcaklık, konsantrasyon, yüzey sürtünme katsayısı, Nusselt ve Sherwood sayıları üzerindeki etkileri ayrıntılı olarak tartışılmaktadır. Manyetik alan ve emme parametreleri arttıkça hızın düştüğü bulunmuştur. Ayrıca emme sayısı arttıkça sıcaklık ve nanopartikül konsantrasyonu azalır, ancak difüzyon termo ve termal yayılma parametreleri yükseldikçe artar. Richardson ve Prandtl sayılarındaki artış, cilt sürtünmesinin azalmasına ve ısı aktarım hızının artmasına neden olur. Bu çalışmanın sonuçları, endüstriyel ve bilimsel uygulamalarda karşılaşılan çeşitli sistemlerin tasarımını, işletimini ve performansını geliştirmek için kullanılabilir.

1. Introduction

Fluid flows exposed to magnetic fields and buoyancy impacts contribute a noteworthy performance in several industrial and engineering applications such as in the heat exchangers, chemical processes, and materials processing. The comprehension and control of such flows are vital for improving the proficiency and optimizing system performance. Efforts geared towards the exploration of the performance of magnetohydrodynamic (MHD) mixed convection flows, which involves the combined effects of forced and natural convections, as well as magnetic fields shows an increasing trajectory. In MHD mixed convection flows, two substantial physical phenomena namely, cross-diffusion and suction effects perform fundamental roles. The phenomena were diverse species within a fluid display

variable diffusion coefficient, which leads to disparities in concentration profiles and transport properties is termed Cross-diffusion. Meanwhile, suction encompasses the local exclusion of fluid from specific areas in a system, ensuing in modifications to flow configurations and overall fluid behavior. Thus, the scientific significance of suction in fluid dynamics is noteworthy. Firstly, by controlling the suction, scientists and engineers can handle the flow velocity, temperature, and nanoparticle (specie) concentrations in various applications. For example, in cooling systems, the adjustment of suction can aid in regulating fluid velocities and temperatures thereby ensuring optimal cooling efficiency. Secondly, in nanoparticle dispersion processes, the controlling of suction allows for precise control over nanoparticle concentrations in any desired region in a given system. Hence, understanding the impacts of suction will facilitates the configuration and increase in efficiency of fluid flow systems in numerous fields, such as engineering, environmental sciences, and nanotechnology.

The augmentation of heating or cooling is an important aspect in the industrial processes. This is because of its support and contribution in energy saving and optimal performance efficacy of industrial machineries such as, gas turbines. Similarly, some systems are also affected through thermal enrichment processes, thus, the designing, expansion and improvement of high performance thermal transferal systems become necessary. Thus, the introduction of new forms of heat transmission fluidics such as nanofluid becomes very vital. Meanwhile, nanofluidics occurs in form of single and multi-phase fluids. They're composite of convectional fluids existing as H_2O, engine oil, EGC etc., with finely divided and suspended particles of metals and their oxides (nanoparticles) with sizes less than 100 nanometer (nm). However, nanoparticles exist in two forms, namely: soft and hard forms. It can also appear as nanotubes, nano-chips, CNTs etc. Interestingly, Bhattacharyya (2012), examined the characteristics of steady flow and reacting mass transmission over an exponentially elastic plate in a moving fluid. He applied the fourth-order Runge-Kutta and shooting methods in his solution approach. His findings revealed that a rise in Schmidt and reaction rate parameters leads to an increase in mass transport. Liu et al. (2013), have explored three dimensional (3D) boundary wall layer flow and thermal transference of viscous stream over an exponentially expanding sheet. They employed the Ackroyd technique and Runge-Kutta integration scheme in solving their converted equations. Their result opined that thermal transferal characteristics are dependent on the temperature exponent, expanding and Prandtl factors. Several scholars (Nadem et al., 2014), Bhattacharyga & Layele (2014), Mukhopadhyay et al. (2014), Ene & Marinca (2015) have investigated various facet of nanofluidic flow past exponentially extending surface under different constraints. Meanwhile, Das (2012), studied the dual impact of mixed thermophoresis and chemical reaction on MHD micropolar stream for varying fluid properties. The analysis of micropolar fluidic flow and thermal transferal past a lessening plate was conducted by Turkyilmazoglu (2014). His result showed that the

existence of physical structures of micro-rotation and energy profiles appeared either in unique or many forms. The MHD influence on boundary flow with absorbent material over an exponentially contracting surface and slip was examined by Jain & Choudhary (2015). By utilizing the Runge-Kutta and shooting schemes, they noted that the shear stress augments while the velocity and temperature lessens as slip number improves. Similarly, Fauzi et al. (2012), analyzed the mixed convective flow of nanofluids with a leaky upright cone. They obtained twofold solutions for some values of mixed convective factor by adopting the shooting procedure. The examination of thermal transference in mixed convection stream of nanoliquids past a parallel circular cylinder was studied by Rabeti (2014). He maintained that the immersed nanoparticles in the convectional fluid increase the thermal distribution from the cylinder when the non-free convection heat circulation is the leading regime of such thermal transport. Several scientists such as Ali & Al-Yousef (2004), Dandapat et al. (2004), Abo-Eldahas & Abd El-Aziz (2005), Abd El-Aziz & Salem (2007), have explored on heat and mass transportation of a steady stream with a half-infinite fluid layer being controlled by an unceasing expanding plate.

The effect of cross-diffusion and suction on MHD mixed convection flows has fascinated substantial interest owing to their prospect, to meaningfully modify flow characteristics, thermal transmission rates and general system optimal efficiency. Even with their practical significance, an in-depth comprehension of their combined impacts on MHD fluid flow remains incomplete. Lately, Abd El-Aziz (2009, 2010), stretched the work of Elbashbeshy & Bazid (2004), by considering heat radiation, Hall currents and chemical reactivity under bounded time-dependent conditions. They opined that the heat transfer proportion was enhanced as radiation and Prandtl numbers rises. Similarly, Bachok et al. (2011), investigated the similarity resolution of unsteady wall flow and heat conveyance due to a stretching plate. The scrutiny of Soret dissipation effect on heat and mass transfer involving non-newtonian radiative nanofluid flow due to Lorentz drag and Rosseland radiation was reported by Awucha & Okechukwu (2022). They applied the series approximation method in obtaining the analytical result and utilized the Mathematica software in realizing the numerical solutions. According to their finding, increasing the Casson number begets a reduction in velocity and an increase in temperature.

The originality of this study lies in its holistic approach to investigating a complex fluid flow problem. While there are existing studies on MHD flows past various types of plates and surfaces, few combined the Dufour, exponential stretching, suction, and Richardson effects into a single analysis. Thus, by taking all the aforementioned phenomena into consideration in this present study, this research bridges the gaps in the knowledge and provides a more accurate representation of real-world scenarios, making it highly relevant to practical applications in engineering, physics, and environmental science. The insights gained from this study can lead to the development

of more efficient systems and processes in industries where MHD flows and diffusion effects play a critical and advance role. The current status of the study in the literature provides a brief review of related literature, highlighting previous research on MHD flows past different types of surfaces and plates. Some of the referenced studies explored factors such as temperature gradients, chemical reactions, and nanoparticle dispersion in various flow configurations. The present study identifies a gap in the literature concerning the combined effects of Dufour, cross-diffusion (Richardson), and suction on MHD convective flows. Despite the practical relevance of these phenomena, a comprehensive understanding of their combined impacts remains incomplete. Hence, the primary goal of this study is to develop a mathematical model that analyzes the interplay of physical parameters between Dufour, Richardson, and suction effects on MHD convection flows. The governing models include continuity, conservation, energy transport, and concentration equations. These models will be explored using numerical and computational techniques to gain insights into the flow behavior and heat transportation. The study aims to contribute to the advancement of fundamental knowledge in the field of MHD mixed convection control and provide insights for the designing and optimization of systems involving fluid flows subjected to magnetic fields, buoyancy effects, and controlled mechanisms, thereby enhancing energy efficiency and heat transfer rates. The findings of this study could also have implications in various fields, such as engineering, environmental science, nanotechnology, and biology. The breakdown of the current developments in the literature is as follows:

Significance of MHD and Buoyancy Effects: The text highlights the significance of fluid flows exposed to magnetic fields and buoyancy impacts in various industrial applications, such as heat exchangers, chemical processes, and materials processing. This emphasizes the importance of understanding and controlling these flows for optimizing system performance.

MHD Mixed Convection Flows: The literature has seen an increasing interest in the exploration of magnetohydrodynamic (MHD) mixed convection flows. These flows involve the combined effects of forced and natural convections, as well as magnetic fields. Researchers are recognizing the practical relevance of these flows and their potential to enhance system efficiency.

Role of Cross-Diffusion and Suction: In MHD mixed convection flows, two fundamental physical phenomena, namely cross-diffusion and suction effects, play significant roles. Cross-diffusion involves diverse species within a fluid with variable diffusion coefficients, leading to variations in concentration profiles and transport properties. Suction, on the other hand, involves the local exclusion of fluid from specific areas in a system, leading to modifications in flow configurations.

Applications of Suction: Suction is highlighted as a valuable tool for controlling flow velocity, temperature, and nanoparticle concentrations in various applications. For instance, it can optimize cooling efficiency in cooling systems and enable precise control over nanoparticle concentrations in processes like nanofluid dispersion. This study provides an in-depth comprehension of the principles of suction due to its importance in the designing and optimization of proficient systems such as pumps, turbines, and ventilation systems. In biological systems, the principle of suction remains vital for processes such as respiration, feeding, and circulation. Furthermore, it is engaged in medical applications like wound healing, drug delivery, and blood collection. In addition, the mixed convection plays an integral role in different applications such as in the designing of heat exchangers, cooling systems for electronic devices, and thermal management for industrial processes. It also has implications in environmental phenomena, such as the dispersion of pollutants in the atmosphere and the movement of heat and mass in natural water bodies. However, the current deficiencies in the literature include:

Limited Understanding of Combined Effects: Despite the growing interest in MHD mixed convection flows, the text highlights that there is still an incomplete understanding of the combined impacts of cross-diffusion and suction on these flows. This is a gap in the literature that needs to be addressed.

Scope of Previous Research: Previous studies have primarily focused on individual aspects of fluid flow and heat transfer, such as radiation, chemical reactivity, or nanoparticle dispersion. However, there is a lack of comprehensive research that considers the combined effects of cross-diffusion, suction, and other factors in MHD flows.

Unexplored Interactions: The text emphasizes that the interactions between Richardson flow, cross-diffusion, and suction effects in MHD mixed convection flows have not been thoroughly explored. These interactions have the potential to significantly modify flow characteristics and thermal transmission rates.

Proposed Study's Contributions: The proposed study aims to bridge the existing gaps in the literature by developing a mathematical model that accounts for the interplay of physical parameters related to Richardson flow, cross-diffusion, and suction effects in MHD mixed convection flows. By conducting a detailed analysis using numerical and computational techniques, the study intends to provide insights into flow behavior and heat transfer under the influence of Dufour, Soret, and suction parameters.

2. Materials and Method

2.1. Mathematical formulation

A steady, laminar and incompressible mixed convection flow of an electrically conducting nanofluidic due to heat and mass transmission past a partially infinite plate imbedded in a fluid is considered. It is assumed that the flow is in vertical direction along the plate in $x - axis$ and normal in the $y -$axis. The plate is kept at temperature $T_s(x)$ and concentration $C_s(x)$ with baseline temperature and concentration expressed as $T_\infty(x)$ and $C_\infty(x)$ respectively. However, the physical geometry of the model is depicted in Figure 1.
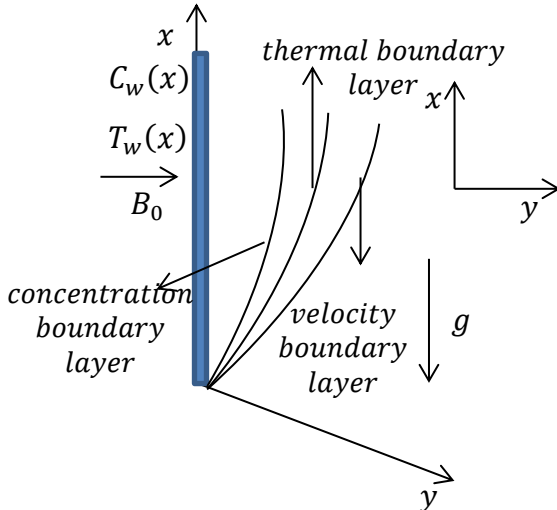
Figure 1. Schematic flow representation

In view of the aforementioned conditions and under the Boussinesq's approximations (1877), the governing boundary layer models are presented below:

2.1.1. Continuity equation

$$\frac{\partial v'}{\partial y'} = 0 \tag{1}$$

2.2.1. Momentum conservation equation

$$\frac{\partial p'}{\partial x'} + u\frac{\partial u'}{\partial x'} + v\frac{\partial u'}{\partial y'} = v\frac{\partial^2 u'}{\partial y'^2} + \frac{g\lambda^*(T-T_\infty)}{Re_x^2} - \frac{\sigma B_O^2 u'}{\rho} \tag{2}$$

2.3.1. Energy conservation equation

$$\frac{\partial T'}{\partial x'} + v\frac{\partial T'}{\partial y'} = \frac{1}{\rho C_p}\frac{\partial}{\partial y'}\left(k\frac{\partial T'}{\partial y'}\right) + \ldots$$

$$\frac{DK_T}{C_s C_p}[(C_s - C_\infty)\theta(\eta)] - \frac{k}{\rho C_p}\frac{\partial q_r}{\partial y'} \tag{3}$$

2.3.1. Mass concentration equation

$$u\frac{\partial C'}{\partial x'} + v\frac{\partial C'}{\partial y'} = D\frac{\partial^2 C'}{\partial y'^2} + \frac{DK_c}{T_\mu}(T - T_\infty)\theta(\eta) \tag{4}$$

Under the following boundary constraints

at $y = 0; u(x) = U, v = -V(x), T = T_s, \quad C = C_s$ (5)

as $y \to \infty, u \to 0, T \to T_\infty, C \to C_\infty$ (6)

The suction velocity normal to the sheet is given as

$$v = -V(x) \tag{7}$$

where the components of velocities in both x and y directions are represented by u and v, v is the kinematic viscosity, $p =$fluid pressure,

$k =$ thermal conductance of fluid, $q_r =$ heat flux radiation, $C_p =$specific heat at constant pressure, $D =$ mass diffusivity coefficient, $g =$ acceleration due to gravity, $Re_x =$ local Reynolds number dependent on the sheet velocity, $\lambda^* =$ characteristic length, $\rho =$ fluid density, $\sigma =$electrical conductance,

$k_T =$ proportion of thermal diffusivity,

$K_c =$ mass diffusivity proportion, the negative sign specifies that the suction velocity is in the direction of the plate. According the Rosseland estimation (1936) in terms of q_r, we have

$$q_r = -\frac{4\sigma^*}{3k^*}\frac{\partial T'^4}{\partial y'} \tag{8}$$

where σ^* representing the Stefan-Boltzman term expressing the relationship between the thermal radiation emitted by the sheet,

$T =$ absolute temperature and $k^* =$ mean absorption estimation. Under the condition that the temperature gradient surrounded by the flow exist in such a way that T'^4 can be stated as a linear grouping and with the aid of Taylor series by expanding T'^4 at T_∞ , we got

$$T'^4 = T_\infty'^4 + 4T_\infty'^3(T' - T_\infty') + 6T_\infty'^2(T' - T_\infty')^2 + \cdots \tag{9}$$

By excluding terms of greater orders that are higher than the first degree in $(T' - T_\infty')$, we have

$$T'^4 = -3T_\infty'^4 + 4T_\infty'^3 T' \tag{10}$$

Taking the derivative of Eq. (8) with respect to y' and using Eq. (10) produces

$$\frac{\partial q_r}{\partial y'} = -\frac{16T_\infty^3 \sigma^*}{3k^*}\frac{\partial^2 T'}{\partial y'^2} \tag{11}$$

Putting Eq. (11) into Eq. (3) leads to

$$u\frac{\partial T'}{\partial x'} + v\frac{\partial T'}{\partial y'} = \frac{1}{\rho C_p}\frac{\partial}{\partial y'}\left(k\frac{\partial T'}{\partial y'}\right) + \frac{DK_T}{C_s C_p}[(C_s - C_\infty)\theta(\eta)] - \frac{16T_\infty^3 \sigma^*}{3k^*}\frac{\partial^2 T'}{\partial y'^2} \tag{12}$$

Introducing the stream functions, $u = \frac{\partial \psi}{\partial y}$ and

$v = -\frac{\partial \psi}{\partial x}$ into Eq. (1) shows that it is satisfied. Since the pressure is a constant, we have

$$\frac{\partial p'}{\partial x'} = 0 \tag{13}$$

In order to transform Eq. (2), (4) and (16) into a coupled ordinary differential equations, the following relevant transformation variables are defined accordingly as

$$\eta = y\sqrt{\frac{U_0}{2vL}}\, e^{\frac{x}{2L}}$$

$$u = U_0 e^{\frac{x}{2L}}\frac{df}{d\eta} \tag{14}$$

$$v = -\sqrt{\frac{vU_0}{2L}}\, e^{\frac{x}{2L}}\left[\left(f(\eta) + \eta\frac{df}{d\eta}\right)\right]$$

$$T = T_\infty + T_0 e^{\frac{x}{2L}}\theta(\eta)$$

Putting Eq. (14) into Eq. (2), (4), (16) and simplifying produces

$$\frac{d^3f}{d\eta^3} + f(\eta)\frac{d^2f}{d\eta^2} + \gamma\theta(\eta) - M\frac{df}{d\eta} = 0 \tag{15}$$

$$(1+S)\frac{d^2\theta}{d\eta^2} + Prf(\eta)\frac{d\theta}{d\eta} + D_f\theta(\eta) = 0 \tag{16}$$

$$\frac{d^2\emptyset}{d\eta^2} + Scf(\eta)\frac{d\emptyset}{d\eta} + S_t\theta(\eta) = 0 \tag{17}$$

Subject to the following boundary expressions.

at $\eta = 0$: $f = m_0, f' = 1, \theta = 1, \emptyset = 1$ (18)

as $\eta \to \infty$: $f' \to 0, \theta \to 0, \emptyset \to 0$ (19)

where, $M = \frac{2\sigma B_0^2 l}{\rho U_w}, \gamma = \frac{Gt}{Re_x^2}, Gt = \frac{g\lambda(T_s - T_\infty)l}{v^2}, Re_x = \frac{U_w l}{v},$

$Pr = \frac{v}{\alpha}, D_f = \frac{Dk_t}{C_s C_p}\left(\frac{(C_s - C_\infty)}{(T_s - T_\infty)}\right), S = \frac{16\sigma^* T_\infty^3}{3k^* k}, Sc = \frac{v}{D}$ and

$$S_t = \frac{Dk_c}{T_\mu}\left(\frac{(T_s - T)}{(C_s - C_\infty)}\right)$$

refers to magnetic strength, mixed (Richardson) convective, local Reynolds, Prandtl, Dufour, radiation, Schmidt and Soret parameters respectively. However, $m_0 = \frac{v_0}{\sqrt{\frac{vU_0}{2L}}} > 0$ and $m_0 = \frac{v_0}{\sqrt{\frac{vU_0}{2L}}} < 0$ is indicative of the suction and blowing numbers.

However, the current research was solved analytically by deploying the improved series approximation technique in order to realize the solutions. The steps involve:

It refers to a mathematical method used in finding the approximate solutions for differential equations with a small parameter, denoted by δ. This technique is mainly useful when a given ODE is coupled, complex in nature and cannot be solved directly.

1. The ODE involving a small parameter δ, is written.

2. The solution is assumed in such a way that it can be stated as a sum of an infinite power series such as: $y(\eta) = f_0(\eta) + \delta f_1(\eta) + \delta^2 f_2(\eta) + \cdots$ were $f_0(\eta), f_1(\eta), f_2(\eta),$ etc., are to be found.

3. The assumed solution are used in the original ODE and coefficients of various powers of δ equated.

4. The resulting equations are solved in order to find the expressions for the unknown functions.

5. The obtained values of $f_0(\eta), f_1(\eta), f_2(\eta),$ etc., are substituted into the assumed solution given in the second step above so as to determine the approximate solution, $f(\eta)$.

6. The constants of integration that are present in the solutions already obtained are found by applying the initial or boundary conditions. Thus, the obtained solutions are iterated through simulation with a suitable numerical software.

In accordance with Bestman (1990), the following definitions are utilized to solve Eq. (2), (4) and (16) meaningfully.

$$\eta = \xi m_0, f(\eta) = m_0 F(\eta), \theta(\eta) = w(\eta),$$

$$\emptyset(\eta) = Z(\eta), \omega = \frac{1}{m_0^2} \tag{20}$$

Utilizing Eq. (22) and its differentials into Eq. (15)-(21) and simplifying gives

$$\frac{d^3f}{d\eta^3}(m_0)^4 + f(\eta)\frac{d^2f}{d\eta^2}(m_0)^4 + \gamma\theta(\eta) - M\frac{df}{d\eta}(m_0)^2 0 \tag{21}$$

$$(1+S)\frac{d^2Z}{d\eta^2}(m_0)^2 + Prf(\eta)\frac{dZ}{d\eta}(m_0)^2 + D_f Z(\eta) = 0 \tag{22}$$

$$\frac{d^2W}{d\eta^2}(m_0)^2 + Scf(\eta)\frac{dW}{d\eta}(m_0)^2 + S_t Z(\eta) = 0 \tag{23}$$

$$\eta = 0: f = 1, f' = \omega, Z = 1, W = 1 \tag{24}$$

$$\eta \to \infty: f' \to 0, Z \to 0, W \to 0 \tag{25}$$

By multiplying equations (21) by $\frac{1}{(m_0)^4}$, (22) and (23) by $\frac{1}{(m_0)^2}$, we have the following equations.

$$\frac{d^3f}{d\eta^3} + f(\eta)\frac{d^2f}{d\eta^2} + \gamma Z(\eta)\omega^2 - M\frac{df}{d\eta}\omega = 0 \tag{26}$$

$$(1+S)\frac{d^2Z}{d\eta^2} + Prf(\eta)\frac{dZ}{d\eta} + D_f Z(\eta)\omega = 0 \tag{27}$$

$$\frac{d^2W}{d\eta^2} + Scf(\eta)\frac{dW}{d\eta} + S_t Z(\eta)\omega = 0 \tag{28}$$

$$\eta = 0: f = 1, f' = \omega, Z = 1, W = 1 \tag{29}$$

$$\eta \to \infty: f' \to 0, Z \to 0, W \to 0 \tag{30}$$

As a result of the case of suction, $\omega \ll 1$, the solution of Eq. (26) - (28) is assumed as follows:

$$f(\eta) = 1 + \sum_{j=k=1}^{\infty} \omega^j f_k(\eta) + O(\omega)^3 + \cdots \tag{31a}$$

$$w(\eta) = \sum_{j=k=1}^{\infty} \omega^j Z_k(\eta) + O(\omega)^2 + \cdots \tag{31b}$$

$$z(\eta) = \sum_{j=k=1}^{\infty} \omega^j W_k(\eta) + O(\omega)^2 + \cdots \tag{31c}$$

Differentiating $f(\eta)$ thrice while $w(\eta)$ and $s(\eta)$ are differentiated twice with respect to η, yields the following equations.

$$f'(\eta) = \omega f_1' + \omega^2 f_2' + \cdots$$

$$f''(\eta) = \omega f_1'' + \omega^2 f_2'' + \cdots$$

$$f'''(\eta) = \omega f_1''' + \omega^2 f_2''' + \cdots$$

$$Z' = Z_0' + \omega Z_1' + \cdots \tag{32}$$

$$Z'' = Z_0'' + \omega Z_1'' + \cdots$$

$$W' = W_0' + \omega W_1' + \cdots$$

$$W'' = W_0'' + \omega W + \cdots$$

Putting Eq. (31a, 31b and 31c) and (32) into Eq. (26)-(28) and equating the coefficients of same degrees in zeroth, unity and binary orders in ω^j and further simplification of Eq. (29)-(30) produces the following equations.

Zeroth Order

$$(1 + S)\frac{d^2 Z_0}{d\eta^2} + Pr\frac{dZ_0}{d\eta} = 0; Z_0(0) = 1, \tag{33}$$

$$Z_0(\infty) = 0$$

$$\frac{d^2 W_0}{d\eta^2} + Sc\frac{dW_0}{d\eta} = 0; W_0(0) = 1, W_0(\infty) = 0 \tag{34}$$

Order of Unity

$$\frac{d^3 f_1}{d\eta^3} + \frac{d^2 f_1}{d\eta^2} = 0; f_1(0) = 0, \ f_1'(0) = 1, \ f_1'(\infty) = 0 \tag{35}$$

$$(1 + S)\frac{d^2 Z_1}{d\eta^2} + Pr\frac{dZ_1}{d\eta} + Prf_1(\eta)\frac{dZ_0}{d\eta} + D_f Z_0(\eta) = 0;$$
$$Z_1(0) = 0, \ Z_1(\infty) = 0 \tag{36}$$

$$\frac{d^2 W_1}{d\eta^2} + Sc\frac{dW_1}{d\eta} + Scf_1(\eta)\frac{dW_0}{d\eta} + S_t Z_0(\eta) = 0;$$
$$W_1(0) = 0, \quad W_1(\infty) = 0 \tag{37}$$

Binary Order

$$\frac{d^3 f_2}{d\eta^3} + \frac{d^2 f_2}{d\eta^2} + f_1(\eta)\frac{d^2 f_1}{d\eta^2} + \gamma Z_0(\eta) - M\frac{df_1}{d\eta} = 0;$$
$$f_2(0) = 0, \ f_2'(0) = 0, f_2'(\infty) = 0 \tag{38}$$

Solving the coupled systems of Eq. (33)-(38) with the application of their respective boundary conditions yields the following analytical solutions.

$$f_1(\eta) = 1 - exp - \eta \tag{39}$$

$$f_2(\eta) = exp - \eta + \frac{1}{4}exp - 2\eta + \cdots$$

$$\frac{\gamma}{(A)^2(A-1)}exp - A\eta + M\eta exp - \eta - \cdots$$

$$\frac{\gamma}{(A)^2(A-1)} - \frac{3}{4} + \frac{\gamma}{A(A-1)} - M + \frac{1}{2}exp - \eta - \cdots$$

$$\frac{\gamma}{A(A-1)}exp - \eta + Mexp - \eta \tag{40}$$

$$Z_0(\eta) = exp - A\eta \tag{41}$$

$$Z_1(\eta) = -A\eta exp - A\eta - \frac{(A)^2}{1+A}exp - \cdots$$

$$(1 + A)\eta + \frac{D_f}{Sc(1+S)}\eta exp - A\eta + \frac{(A)^2}{1+A}exp - A\eta \tag{42}$$

$$W_0(\eta) = exp - Sc\eta \tag{43}$$

$$W_1(\eta) = -Sc\eta exp - Sc\eta - \frac{(Sc)^2}{1+Sc}exp - \cdots$$

$$(1 + Sc)\eta + \frac{(Sc)^2}{1+Sc}exp - Sc\eta - \cdots$$

$$\frac{S_t}{A(A-Sc)}exp - A\eta + \frac{S_t}{A(A-Sc)}exp - Sc\eta \tag{44}$$

Therefore, substituting Eq. (39)-(40) into Eq. (31a) gives

$$f(\eta) = 1 + \omega(1 - exp - \eta) + \cdots$$

$$\omega^2\{\eta exp - \eta + \frac{1}{4}exp - 2\eta + \frac{\gamma}{(A)^2(A-1)}exp - A\eta + \cdots$$

$$M\eta exp - \eta - \frac{\gamma}{(A)^2(A-1)} - \frac{3}{4} + \frac{\gamma}{A(A-1)} - \cdots$$

$$M + \frac{1}{2}exp - \eta - \frac{\gamma}{A(A-1)}exp - \eta + Mexp - \eta\} \tag{45}$$

However, the fluid velocity is expressed as

$$F'(\eta) = (m_0)^2 f'(\eta) \tag{46}$$

Thus, we have the analytical solution of the fluid velocity as

$$F'(\eta) = exp - \eta + \frac{1}{(m_0)^2} * \cdots$$

$$\{exp - \eta - \eta exp - \eta - \frac{1}{2}exp - 2\eta - \cdots$$

$$\frac{\gamma}{A(A-1)}exp - .. A\eta - M\eta exp - \eta - \frac{1}{2}exp - \cdots$$

$$\eta + \frac{\gamma}{A(A-1)}exp - \eta\} \tag{47}$$

Again, substituting Eq. (41) - (42) into Eq. (31b) produces the analytical solution of the nanofluid energy transport as

$$Z(\eta) = exp - A\eta + \frac{1}{(m_0)^2}\{-A\eta exp - A\eta - \cdots$$

$$\frac{(A)^2}{1+A}exp - (1+A)\eta + \frac{D_f}{Sc(1+S)}\eta exp - \cdots$$

$$A\eta + \frac{(A)^2}{1+A}exp - A\eta\} \tag{48}$$

Similarly, putting Eq. (43)-(44) into Eq. (31c), gives the analytical solution of the nanoparticle (specie) concentration as presented below.

$$W(\eta) = exp - Sc\eta + \frac{1}{(m_0)^2}\{-Sc\eta exp - Sc\eta - \cdots$$

$$\frac{(Sc)^2}{1+Sc}exp - (1+Sc)\eta + \frac{(Sc)^2}{1+Sc}exp - Sc\eta - \cdots$$

$$\frac{S_t}{A(A-Sc)}exp - A\eta + \frac{S_t}{A(A-Sc)}exp - Sc\eta\} \tag{49}$$

where,

$$A = \frac{Pr}{1+S} \text{ is constant.}$$

The physical quantities of paramount importance for the optimization and designing processes in the engineering, material science and scientific analysis are defined as follows.

$$C_f = \frac{\tau_s^*}{\rho U_0 V_0}, \quad N_{u_x} = x \frac{\left(\frac{\partial T}{\partial y^*}\right)_{y^*=0}}{(T_s^* - T_s^*)} \tag{50}$$

$$S_{h_x} = -x \frac{\left(\frac{\partial C}{\partial y^*}\right)_{y^*=0}}{(C_s^* - C_s^*)}$$

Simplifying Eq. (50) produces the skin-friction, rate of beat transmission (Nusselt number) and Sherwood number (rate of mass transportation) as follows:

$$C_f = -\left(\frac{\partial u}{\partial y}\right)_{y=0} \tag{51}$$

$$f''(\eta) = (m_0)^3 F'' \tag{52}$$

$$f''(0) = -m_0 + \frac{1}{m_0}\left(-\frac{1}{2} + \frac{\gamma}{A-1} - M - \frac{\gamma}{A(A-1)}\right) \tag{53}$$

Again, the Nusselt number is resolved as

$$\frac{Nu}{Re_x} = -\left(\frac{\partial z}{\partial y}\right)_{y=0} \tag{54}$$

$$z'(\eta) = -\left(\frac{\partial z}{\partial y}\right)_{y=0} \tag{55}$$

$$z'(0) = A - \frac{1}{(m_0)^2}\left(-A + (A)^2 + \frac{D_f}{Sc(1+Sc)} - \frac{(A)^2}{1+A}\right) \tag{56}$$

Similarly, the Sherwood number follows:

$$\frac{Sh}{Re_x} = -\left(\frac{\partial w}{\partial y}\right)_{y=0} \tag{57}$$

$$w'(\eta) = -\left(\frac{\partial w}{\partial y}\right)_{y=0} \tag{58}$$

$$w'(\eta) = -Sc + \frac{1}{(m_0)^2}\left\{-Sc + (Sc)^2 - \frac{(Sc)^3}{1+Sc} + \cdots \right.$$

$$\left. \frac{S_t}{A-Sc} - \frac{Sc(S_t)}{A(A-Sc)}\right\} \tag{59}$$

Where, the local Reynolds factor due to the sheet's suction velocity is described as $Re_x = \frac{U_w l}{v}$.

3. Findings and Discussion

Having solved the problem analytically, we have deployed the Wolfram Mathematica software for realizing the numerical results which have been displayed graphically from Figures 2-13 and in Tables 1-3, respectively.

In the study of fluid dynamics, the fluid velocity has the tendency to decline as the magnetic field strength parameter rises owing to a phenomenon termed magnetohydrodynamic (MHD) drag. Meanwhile, in a conductive fluid flow along the direction of a magnetic field, the interaction between them spawns electric currents in the fluid, thus creating its own magnetic fields. These self-generated magnetic fields resist the applied magnetic field, thereby leading to a resistance to the fluid motion. This resistance manifests as an increase in drag, which impedes the fluid's passage and results to a decrease in velocity as the magnetic field strength increases. This phenomenon is displayed in Figure 2. In Figure 3, the influence of mixed convection parameter on the fluids' rate of flow is shown. As this parameter increases, the comparative impact of forced convection becomes more pronounced in relation to natural convection. Thus, this breeds a general increase in velocity within the fluid regime. As a result of this, the improved forced convection component, determined by the external force, transmits enormous momentum to the fluid, resulting in higher velocities and increased fluid motion. The effect of suction parameter, mo on velocity, temperature, and nanoparticle concentrations are illustrated in Figures 4, 5 and 6 respectively. The removal of fluid from the system forms a negative pressure gradient which resists the flow direction thereby countering the natural motion of the fluid and resulting in a decrease in velocity. Hence, the higher the suction parameter, the more significant the deceleration of fluid flow becomes. This phenomenon leads to lessening of the velocity. However, the extraction of fluid begets the loss of heat energy and causes a drop in temperature. The extraction of fluid by suction lessens the overall thermal energy content of a given system and creates a cooling effect. Thus, a rise in suction contributes to a decrease in temperature (energy) in the fluid flow. Similarly, the dispersal of nanoparticles in the fluid is affected by the suction mechanism. As fluid is extracted, the concentration of nanoparticles decreases uniformly. This is because the suction selectively eliminates fluid along with the immersed nanoparticles. Therefore, increasing suction results in a decrease in nanoparticle concentrations within the fluid flow as shown in Figure 6.
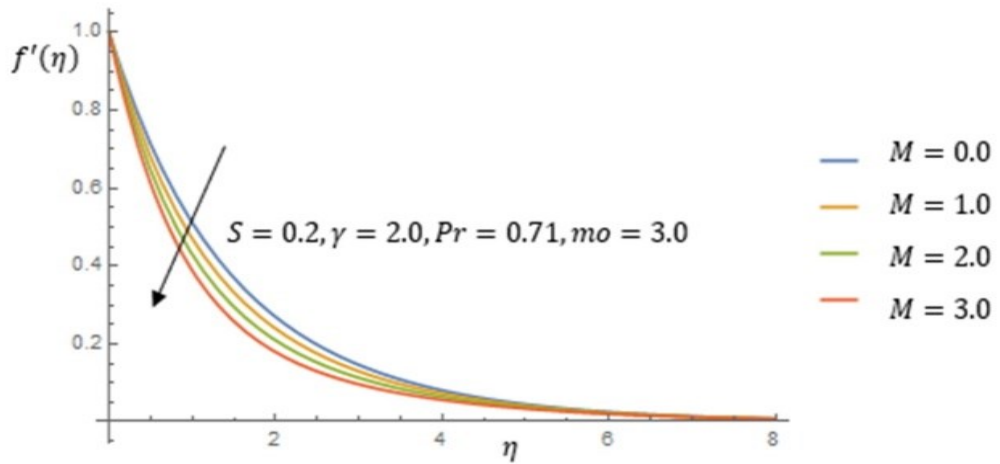
Figure 2. Impact of magnetic field strength, M on the rate of flow (velocity)
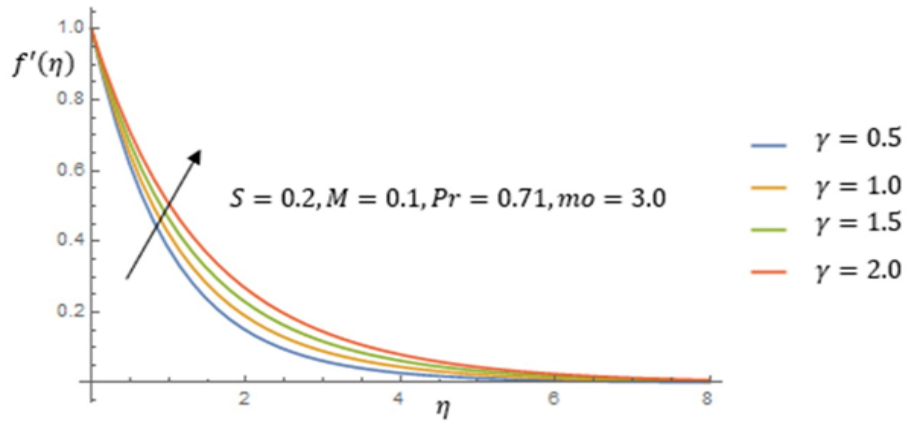
Figure 3. Impact of Richardson (mixed convective) parameter, γ on the rate of flow (velocity)
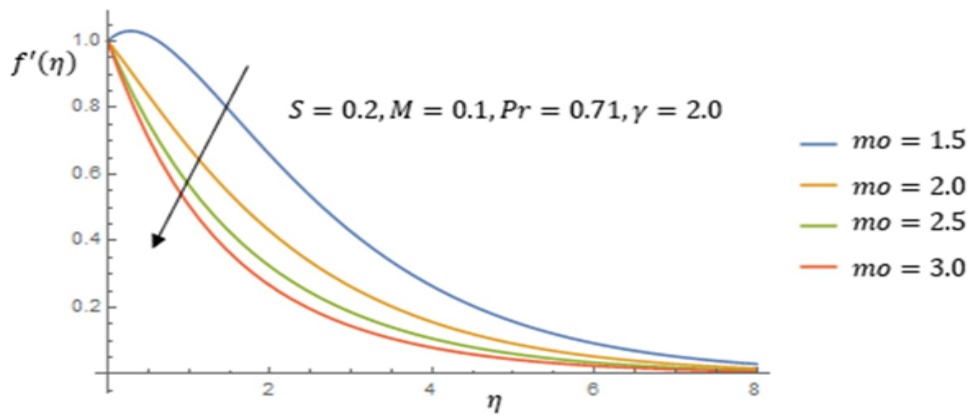
Figure 4. Impact of suction number, m_o on the rate of flow (velocity)
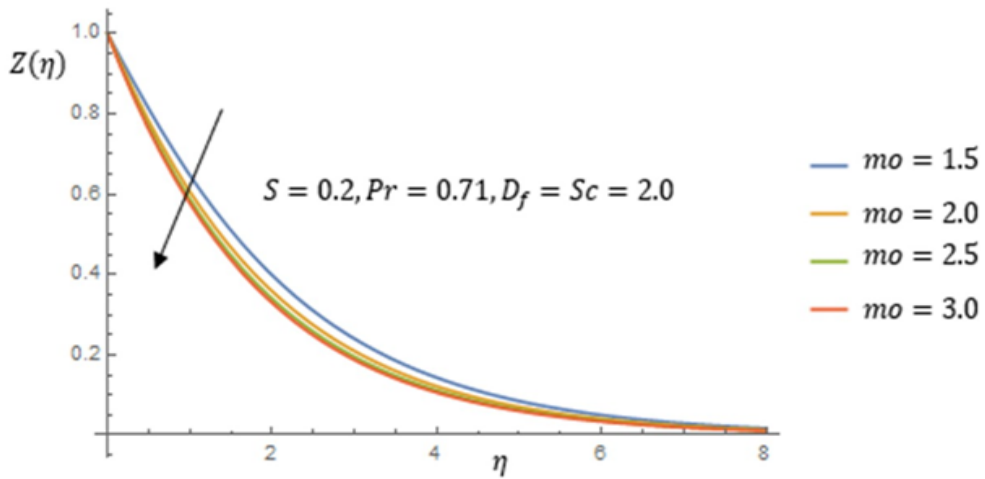
Figure 5. Impact of suction number, m_o on energy (temperature)
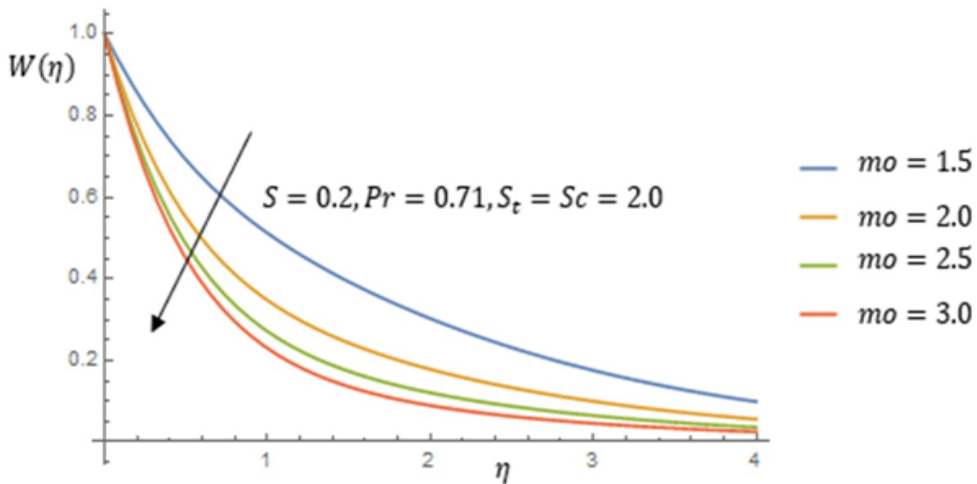
Figure 6. Impact of suction number, m_o on nanoparticle (specie) concentration

The radiation (S) parameter shows a noteworthy role in fluid flow, mainly when considering radiative heat transfer. Thus, its impact on velocity and temperature in the fluid is depicted in Figures 7 and 8. In radiative heat transfer, exchange of energy takes place between the fluid and its surroundings through electromagnetic radiation. Thus, the presence of radiation in the fluid proves the relative significance of radiative heat transferal compared to conduction or convection. When radiation rises, the impact of radiative heat transmission becomes more noticeable and leads to an increased energy transferal from the fluid to its surroundings.

Consequent upon this, the fluid exhibits an alteration in momentum, resulting to an increase in velocity. Similarly, radiative heat circulation can deposit or remove extra energy in or out of the fluid, depending on the temperature differences between the fluid and its walls. Therefore, when the S increases, the radiative heat motion becomes more prevailing and the energy interchange through radiation signifies a greater impact on the fluid temperature. Hence, this leads to a surge in the fluid's temperature.
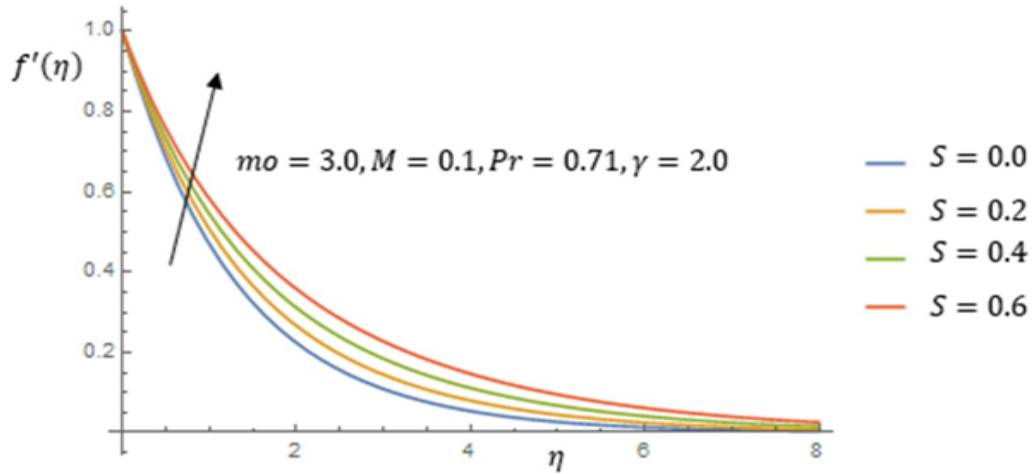
Figure 7. Impact of radiation parameter, S on the rate of flow (velocity)
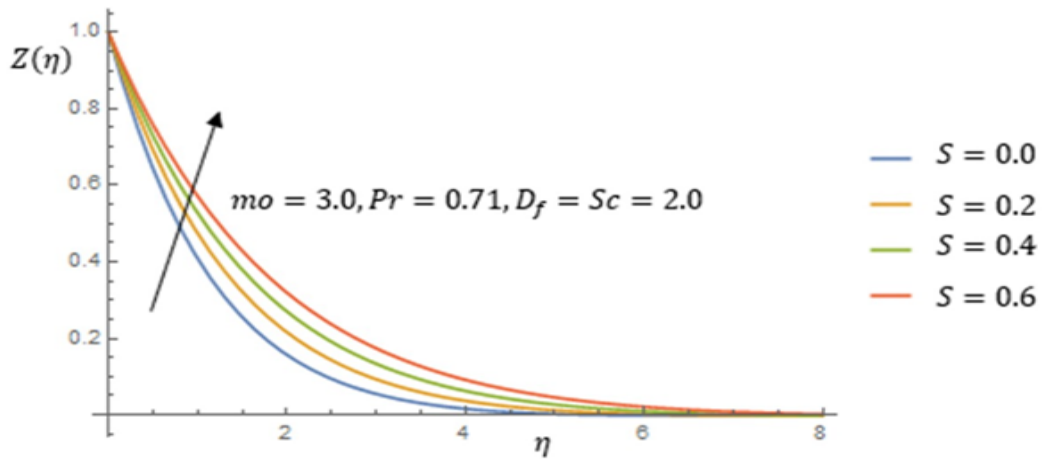
Figure 8. Impact of radiation parameter, S on energy (temperature)

The effects of Dufour (Df) and Soret (S_t) parameters on temperature and nanoparticle concentration are demonstrated in Figures 9 and 10. Meanwhile, both of them play critical roles in heat and mass transmission. Generally, Df enumerates the relative significance of thermal diffusivity associated with convective heat transmission. As it grows, the importance of thermal diffusion becomes evident as it leads to an augmented connection between the temperature and mass concentration. Thus, this breeds a surge in the temperature of the system. This process possesses numerous applications to combustion processes, chemical reactivity and thermal exchangers. Correspondingly, the S_t parameter quantifies the significance relation of thermal transfer which is likened to the solute diffusion. As it rises, the impact of thermal distribution appears more momentous and leads to a distinct Soret influence. This effect begets superior dispersal of a given component over another because of energy differences. Accordingly, an increase in nanoparticle concentration gradients of the fluid occasioning a higher concentration of the solute in

certain areas remains obvious. Thus, the significance of this parameter in this study is vital in the areas of chemical engineering, geophysics and environmental science where exact prediction and control of mass concentration distributions are essential.

In figures 11 and 12, the impact of the non-dimensional numbers i.e., Prandtl (Pr) and Schmidt (Sc) are demonstrated. The Prandtl number relays the ratio of momentum diffusion (viscosity) to heat dispersal. Thus, heat energy disperses gradually when equated to dissipation of momentum thereby leading to a reduction in the temperature gradient. The implication of this effect in different areas includes thermal transmission processes which involve the control of energy variations and it is critical for boosting system efficiency and thermal stresses prevention. Thus, an enhanced Pr shows that the fluid possesses a moderately little thermal diffusion in relation to its viscosity. Similarly, the Schmidt number involves the ratio of momentum diffusion (viscosity) to mass diffusion. However, an improved Sc indicates that a

fluid has a reasonably small mass diffusion in comparison to its viscosity. Owing to this fact, the dispersion of nanoparticles or its concentration differences happens at a gradual pace in relation to momentum circulation. Hence, this ushers decline in nanoparticle concentration distribution in the flow. The worth of Schmidt number is crucial in mass

transportation as it applies to chemical reactions and pollutant dispersal.
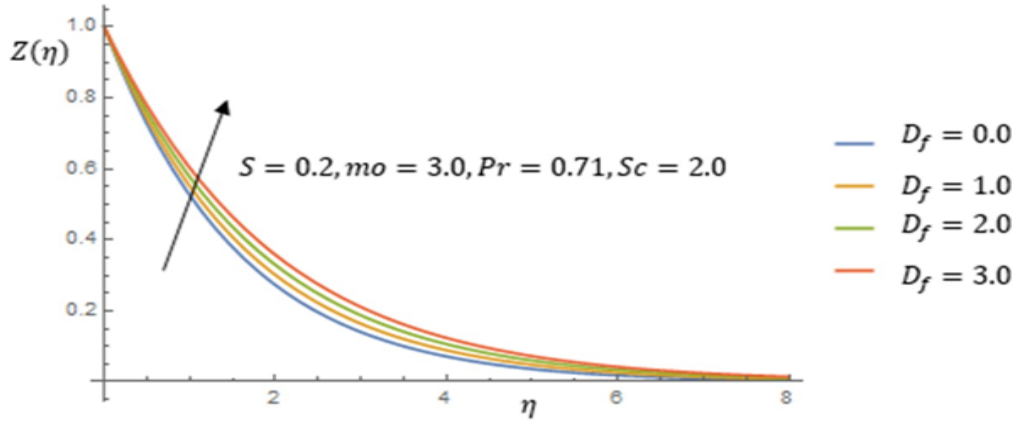
Figure 9. Impact of Dufour number, D_f on energy (temperature)
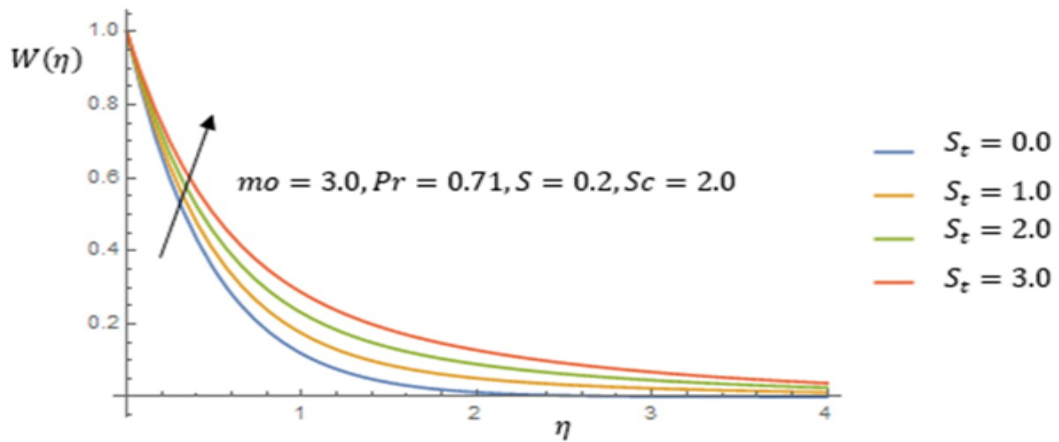
Figure 10. Impact of Soret number, S_t on nanoparticle (specie) concentration
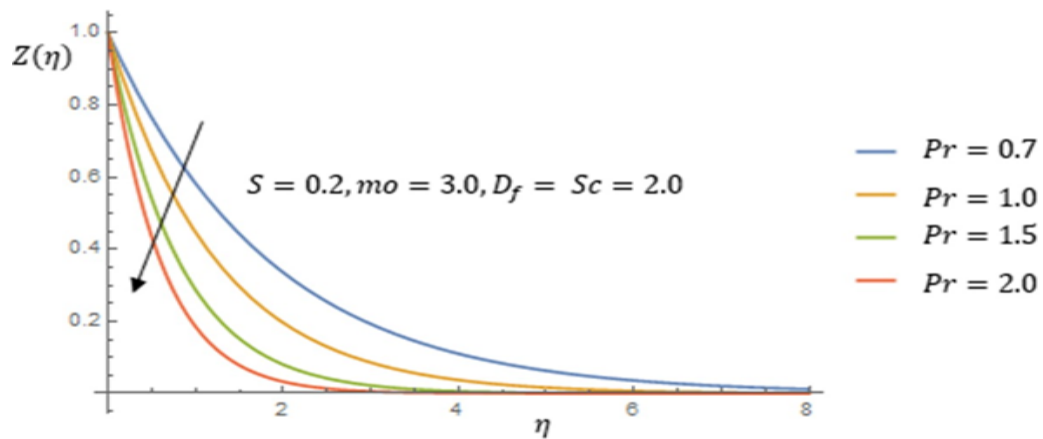
Figure 11. Impact of Prandtl number, Pr on energy (temperature)
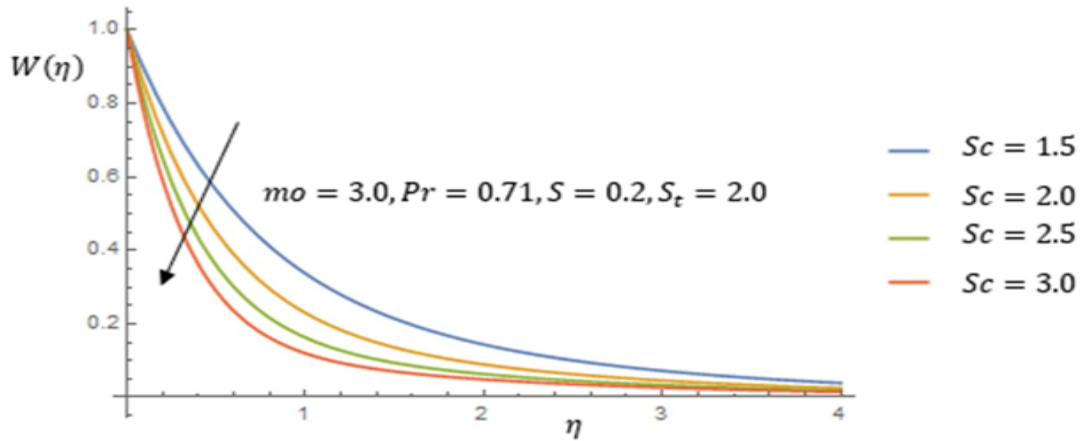
Figure 12. Impact of Schmidt number, Sc on nanoparticle (specie) concentration

The effects of suction, mixed convection and radiation on the skin friction are shown in Table 1. As the fluid is extracted from a system, its flowing momentum declines, thereby causing an increase in the interaction and resistance between the fluid and its boundary walls. Thus, an increase in suction leads to a corresponding increase in the skin friction. Conversely, the increasing effect of the mixed convective parameter, which consists of forced and natural convections, begets a shrinking condition in the skin friction because the forced convection component which is controlled by an applied force, improves the fluid motion close to the wall, thereby decreasing the thickness of the boundary layer and reducing skin friction. Also, as radiation improves, the radiative heat dispersal appears more pronounced as it aids in the cooling of the fluid close to the wall by lowering the temperature differences and accordingly diminishing skin friction. In Table 2, the impacts of the suction, Prandtl and radiation parameters on the rate of heat distribution (Nusselt number) are displayed. However, as suction increases, more fluid is loss from the system and the convective heat transport between the solid wall and the residual fluid becomes stronger, thus leading to a greater thermal transportation and increased Nusselt number. On the contrary, the Prandtl number has a crucial influence on the Nusselt number. This is because an improved Prandtl number signifies a relatively smaller thermal diffusivity in relation to viscosity, which brings about a drop in the temperature of the fluid. However, close to the wall, the convective heat dispersal rate lessens and eventually leads to a decrease in the Nusselt number. On the other hand, as the radiation parameter rises, the radiative heat distribution becomes more noticeable, and produces extra heat exchange between the solid wall and surrounding fluid through electromagnetic radiation.

The effect of suction, Schmidt and Soret parameters on the Sherwood number are presented in Table 3. The Sherwood number signiifies the mass transfer rate from the plate's surface to the immediate fluid. As fluid extraction takes place in the system, the mass transmitance between the sheet and residual fluid turns to be more distinct, and causes an enhanced mass transfer and a developed Sherwood number. Thus, an enhancement of this number produces an increment in the rate of mass transfer. On the contrary, the radiation parameter which is related to radiative thermal allocation shows a dissimilar result on the Sherwood number as it impact on the mass transferal rate. Hence, as it increases, the effect of radiative heat transfer becomes obvious. Therefore, as the radiative heat transfer influences the concentration gradients close to the solid surface and changes the mass transfer rate, the concentration gradients drops while the mass circulation rate decreases, thereby resulting in a lower Sherwood number.

Table 1. Effect of suction, mixed convection and radiation constraints on skin friction at $M = 0.1, Pr = 0.71$

S	γ	m_O	$f''(0)$
0.2	2.0	1.5	-0.3535
0.2	2.0	0.2	0.6099
0.2	2.0	2.5	1.3879
0.2	2.0	3.0	2.0732
0.2	0.5	3.0	2.9183
0.2	1.0	3.0	2.6366
0.2	1.5	3.0	2.3549
0.2	2.0	3.0	2.0732
0.0	2.0	3.0	2.2610
0.2	2.0	3.0	2.0732
0.4	2.0	3.0	1.8855
0.6	2.0	3.0	1.6977

Table 2. Effect of Dufour, Prandtl and suction constraints on Nusselt number (rate of thermal conveyance) at $S = 0.2, \ Sc = 2.0$

D_f	Pr	m_O	$-\theta'(0)$
0.0	0.71	3.0	0.6329
1.0	0.71	3.0	0.5867
2.0	0.71	3.0	0.5404
3.0	0.71	3.0	0.4941
2.0	0.7	3.0	0.5317
2.0	1.0	3.0	0.7912
2.0	2.0	3.0	1.6435
2.0	3.0	3.0	2.4868
2.0	0.71	1.5	0.3865
2.0	0.71	2.0	0.4763
2.0	0.71	2.5	0.5178
2.0	0.71	3.0	0.5404

Table 3. Effect of suction, Schmidt and Soret numbers on Sherwood number (rate of mass distribution) at $S = 0.2, \ Pr = 0.71$

S_t	m_O	Sc	$-\varnothing'(0)$
2.0	1.5	2.0	0.7939
2.0	2.0	2.0	1.3216
2.0	2.5	2.0	1.5658
2.0	3.0	2.0	1.6985
2.0	3.0	1.5	1.1911
2.0	3.0	2.0	1.6985
2.0	3.0	2.5	2.2038
2.0	3.0	3.0	2.7078
0.0	3.0	2.0	2.0741
1.0	3.0	2.0	1.8863
2.0	3.0	2.0	1.6985
3.0	3.0	2.0	1.5107

4. Conclusion

Having examined the analysis of MHD convective stream over an exponentially expanded infinite plate with suction and cross-diffusion impacts, the following conclusions are reached.

1. An increase in mixed convective and radiation parameters $\gamma = 0.5, 1.0, 1.5, 2.0$ and $S = 0.0, 0.2, 0.4, 0.6$, begets a rise in velocity and temperature.

2. Enhancement of Dufour, $D_f = 0, 1, 2, 3$ and Soret $S_t = 0.0, 1.0, 2.0, 3.0$ numbers leads to a surge in temperature and concentration.

3. The improvement of the skin-friction, Nusselt (heat transfer rate) and Sherwood numbers (mass transference rate) is as a result of increasing suction $mo = 1.5, 2, 2.5, 3$ parameters.

4. An upsurge in Dufour number reduces the Nusselt number whereas a rising effect of Soret parameter $S_t = 0.0, 1.0, 2.0, 3.0$ shows a growth in the Sherewood number.

5. A rise in the values of Prandtl factor, $Pr = 0.7, 1.0, 1.5, 2.0$ indicate an increase in the heat transfer rate.

Future Study Recommendations

In line with the current study, the following recommendations are made as areas of future studies.

1. Parametric Studies: The investigation of the sensitivity of the flow characteristics to various parameters is essential. Future studies can explore how changes in vital parameters, such as the magnetic field strength, suction velocity, and diffusion coefficients, affect the flow patterns and boundary layer properties. Thus, understanding the parameter dependencies can guide engineers and researchers in optimizing real-world applications.

2. Multiscale Modeling: The consideration of multiscale modeling approaches that incorporate both macroscopic and microscopic phenomena is vital. However, Cross-diffusion effects often involve interactions at the molecular level, while MHD flow is a macroscopic phenomenon. Future research can explore how to bridge the gap between these scales to develop more accurate and comprehensive models for practical scenarios where both effects are present.

Funding

Conflict of Interest

The authors did not mention any conflict of interest.

Acknowledgement

Nomenclature

CNTs	Carbon nanotubes
MHD	Magnetohydrodynamic
n_p	Nanoparticle
n_f	Nanofluid
u, v	Velocity components in x and y axe (ms^{-2})
x, y	Coordinates of the horizontal and vertical axes
U	Dimensionless free stream velocity (ms^{-1})
U_w	Velocity at the wall of the plate (ms^{-1})
T_∞	Temperature far from the plate (K)
T_w	Temperature at the exterior of the plate (K)
C_w	Nanoparticle concentration at the wall $(kg\ m^{-3})$
C_∞	Nanoparticle mass far away from the wall $(kg\ m^{-3})$
T	Fluid temperature (K)
D_T	Coefficient of thermophoresis
D_m	Coefficient of mass diffusivity $(m^2 s^{-1})$
η	Similarity variable
f'	Dimensionless velocity
θ	Non-dimensional temperature
$\emptyset$	Dimensionless concentration.

5. References

Abd El-Aziz, M. (2009). Radiation effect on the flow and heat transfer over an unsteady stretching sheet. *International Communications in Heat and Mass Transfer, 36*, 521-524.

Abd El-Aziz, M. (2010). Flow and heat transfer over an unsteady stretching surface with Hall Effect. *Meccanica, 45*, 97-109.

Abd El-Aziz, M., & Salem, A. M. (2007). MHD-mixed convection and mass transfer from a vertical stretching sheet with diffusion of chemically reactive species and space or temperature dependent heat source. *Canadian Journal of Physics, 85*, 359-373.

Abo-Eldahab, E. M., & Abd El-Aziz, M. (2005). Flow and heat transfer in a micropolar fluid past a stretching surface embedded in a non-Darcian porous medium with uniform free stream. *Applied Mathematics and Computation, 162*, 881-899.

Ali, M., & Al-Yousef, F. (2004). Laminar mixed convection boundary layers induced by a linearly stretrching permeable surface. *International Journal of Heat and Mass Transfer, 45*, 4241-4250.

Awucha, U. U., & Okechukwu, A. (2022). Soret dissipation effect on heat and mass transmission of non-Newtonian Casson Radiative nanofluid Flow with Lorentz drag and Rosseland radiation. *Journal of Pure and Applied Sciences, 21*(2), 120-127. https://doi.org/10.51984/jopas.v21i2.2059

Bachok, N., Ishak, A., & Nazar, R. (2011). Flow and heat transfer over an unsteady stretching sheet in a micropolar fluid. *Meccanica, 46*(9), 935-942.

Bestman, A. R. (1990). The boundary-layer flow past a semi-infinite heated porous plate for two-component plasma. *Astrophysics and Space Science, 173*, 93-100.

Bhattacharyya, K. (2012). Steady boundary layer flow and reactive mass transfer past an exponentially stretching surface in an exponentially moving free stream. *Journal of the Egyptian Mathematical Society, 20*, 223-228.

Bhattacharyya, K., & Layek, G. C. (2014). Magnetohydrodynamic boundary layer flow of nanofluid over an exponentially

stretching permeable sheet. *Physics Research International,* 592536. https://doi.org/10.1155/2014/592536

Boussinesq, J. (1877). *Analytical Theory of Heat*. Gauthier-Villars. Paris.

Dandapat, B. S., Singh, S. N., & Singh, R. P. (2004). Heat transfer due to permeable stretching wall in the presence of transverse magnetic field. *Archives of Mechanics, 56*, 87-101.

Das, K. (2012). Influence of thermophoresis and chemical reaction on MHD micropolar fluid flow with variable fluid properties. *International Journal of Heat and Mass Transfer, 55*, 7166-7174.

Elbashbeshy, E. M. A., & Bazid, M. A. A. (2004). Heat transfer over an unsteady stretching surface. *Heat Mass Transfer*, *41*, 1-4.

Ene, R. D., & Marinca, V. (2015). Approximate solutions for steady boundary layer MHD viscous flow and radiative heat transfer over an exponentially porous stretching sheet. *Applied Mathematics and Computation, 269*, 389-401.

Fauzi, E. L. H., Ahmad, S., & Pop, I. (2012). Mixed convection boundary layer flow from a vertical cone in a porous medium filled with a nanofluid. *Journal of Mathematical, Computational, Physical, Electrical and Computer Engineering*, *6*, 10-22.

Jain, S., & Choudhary, R. (2015). Effects of MHD on boundary layer flow in porous medium due to exponentially shrinking sheet with slip. *Procedia Engineering, 127*, 1203-1210.

Liu, I. C., Wang, H. H., & Peng, Y. F. (2013). Flow and heat transfer for three-dimensional flow over an exponentially stretching surface. *Chemical Engineering Communications, 200*, 253-268.

Mukhopadhyay, S., Bhattacharyya, K., & Layek, G. C. (2014). Mass transfer over an exponentially stretching porous sheet embedded in a stratified medium. *Chemical Engineering Communications, 201*, 272-286.

Nadeem, S., Haq, R. U., & Khan, Z. H. (2014). Heat transfer analysis of water-based nanofluid over an exponentially stretching sheet. *Alexandria Engineering Journal, 53*, 219-224.

Rabeti, M. (2014). Mixed convection heat transfer of nanofluids about a horizontal circular cylinder in porous media. *SOP Transaction on Nano Technology, 1*(1), 1-4.

Rosseland, S. (1936). *Theoretical Astrophysics*. Clarendon Press, Oxford.

Turkyilmazoglu, M. (2014). A note on micropolar fluid flow and heat transfer over a porous shrinking sheet. *International Journal of Heat and Mass Transfer, 72*, 388-391.